P2.1

AN OCEAN SURFACE WIND VECTOR MODEL FOR WINDSAT MICROWAVE RADIOMETER USING DUAL-POLARIZATION

Seubson Soisuvarn* and Zorana Jelenak
UCAR NOAA/NESDIS/STAR
Paul S. Chang
NOAA/NESDIS/STAR

1. INTRODUCTION

Ocean surface wind field information is vital for scientists and forecasters for their understanding the Earth's global weather and climate. As the demand for global wind vector information was increasing in the last three decades, number of satellite missions that carried instruments for surface wind measurement were launched. However, there is still not sufficient number of instruments flying simultaneously in orbit to fulfill the operational, meteorological and non-real-time scientific wind vector requirements (Chang and Jelenak, 2006).

Starting from the late 1970's up to the recent years, all ocean surface wind vector missions from space were utilizing scatteromery measurements technique (Moore and Jones, 2004). The scatterometers are microwave radar instruments that measure the ocean surface normalized radar cross-section (NRSC) and infer the wind vector information by comparing NRCS with the Geophysical Model Function (GMF) specifically defined for backscatter measurements. The currently used model function QSCAT-1 was developed empirically using known surface truth and observed NRSC from QuikSCAT scatterometry measurements (Freilich, 1993). Due to biharmonic nature of the GMF, the wind vectors retrieved from the NRSC measurements are not unique. There are up to four possible solutions for each measurement. In order to select correct vector from retrieved wind vector ambiguities NRCS measurements are acquired from multiple looks. (Schroeder et al., 1985; Shaffer et al., 1991)

In January 2003, the Naval Research Laboratory launched the first fully polarimetric passive microwave radiometer - WindSat on board of Coriolis satellite (Gaiser and Bettenhausen, 2005). WindSat is the first passive microwave instrument flown in space capable of measuring ocean surface wind speed and direction. WindSat operates at five frequency bands: 6.8, 10.7, 18.7, 23.8 and 37.0 GHz. The 10.7, 18.7 and 37.0 GHz channel are fully polarimetric establishing all four Stokes parameters and are primary channels used for wind vector retrieval. The 6.8 and 23.8 GHz channels are dual-polarized and are used in conjunction with other channels to retrieve relevant surface and atmospheric parameters that complement the wind vector retrieval requirements.

NOAA/NESDIS WindSat's wind vector retrieval algorithm utilizes an empirical model function that establishes relationship between the third and fourth Stokes parameters and the surface wind truth (Jelenak et at. 2004). Although the principal polarizations (vertical and horizontal) are also functions of wind direction, this dependence is very weak and often masked by other surface or atmospheric parameters. However it has been shown (Meissner and Wentz, 2002) that certain linear combination between the vertical and horizontal brightness temperatures are proved to approximately cancel the atmospheric effect and are predominantly dependent on the sea surface temperature, wind speed and direction. We extended this work and shown that the brightness temperature combinations can be expressed as AT_{BV}-T_{BH} where A is a ratio of the surface reflectivities.

For low to moderate wind speeds the wind direction sensitivity of AT_{BV}-T_{BH} is weak and lies within the measurement noise level. However, the more robust wind direction signal in AT_{BV}-T_{BH} reveals the opportunity to use it in combination with the third and forth Stokes measurements for possible wind vector retrieval improvement for fully polarimetric radiometers. In this paper, we investigate the AT_{BV}-T_{BH} characteristic for the WindSat's 10.7, 18.7 and 37.0 GHz channels and present preliminary model functions for these three WindSat frequencies.

The paper is organized as the following: In section 2, dataset that was used for model function development is described. The dataset was separted into two groups with two different sea surface temperature sources as we will describe in more details below. In section 3, the approximation of the linear combination between the vertical and horizontal brightness temperatures is presented.The A parameter has been derived. Next the empirical relationship has been developed for AT_{BV}-T_{BH} and surface parameters and is presented in section 4. Finally the conclusions and discussion is presented in section 5.

2. DATASET

Several data sources were combined in order to develop new model functions for WindSat measurements. From WindSat, linearly polarized (V and

*Corresponding author address: Seubson Soisuvarn, NOAA Science Center, room 102, 5200 Auth Road, Camp Springs, MD 20746; e-mail: seubson.soisuvarn@noaa.gov

H) brighness temperatures are available from all five frequency channels. To avoid predominent atmospheric sensitivity in the 23.8 GHz and SST sensitivity in 6.8 GHz channel and also to match the frequency use for wind retrieval in WindSat's third and forth Stokes parameters, only 10.7, 18.7 and 37.0 GHz channels were used in the model development together with WindSat's own geophysical retrieval parameters such as: cloud liquid water, rain rate, water vapor, wind speed, and sea surface temperature (SST) (Jelenak et al., 2004).

Collocated wind vector data from SeaWinds scatterometer on QuikSCAT (from now on refer to QuikSCAT wind vectors) were used as a surface wind vector truth. The spacial collocation requirement was set to 25-km and time collocation was within ±1 hr time.

Another external data source was needed for better sea surface temperature (SST) estimates. This parameter was obtained from the National Centers for Environmental Prediction's (NCEP) Global Data Assimilation System (GDAS). The GDAS is a global map model of the Earth's atmosphere and ocean surface generated every 6 hr. for 00Z, 06Z, 12Z and 18Z daily. The current NOAA/NESDIS version of GDAS used provides a 1° × 1° global latitude/longitude grid resolution for a limited selection of parameters significant for satellite geophysical retrievals validation. Since GDAS produce four global maps per day, the closest maps timeframe within ±3 hr of WindSat overpass were selected. Next the closest four surronding points of GDAS were then interpolated to the WindSat point location (Connor, 2004).

All the data from WindSat, QuikSCAT and GDAS sets were combined together in a common data structure to simplify data processing. To make the dataset suitable for model function development, the dataset was binned with respect to different surface parameter as obtained from QuikSCAT or GDAS model field. The dataset was first sorted by QuikSCAT's wind speeds into 1 m/s wind speed bins.

From the wind speed bins, the data were further subdivided into SST bins with 2 °C bin size. It would be desirable to use the derived SST from WindSat alone without using other external SST source like GDAS. To assess the requirement of an external SST source, both SST from WindSat retrievals (Mavor et al, 2004) and GDAS SST was used to bin the data. Here we refer to the two version of dataset as version-1 (ver-1) and version-2 (ver-2) corresponding to SST bins used based on GDAS's and WindSat's respectively.

Finally, these two dimensional wind speed and SST bins, were further divided in to relative wind direction bins of 10° size. The term "relative" refers to the difference between true wind direction and WindSat's measurement azimuth.

3. BRIGHTNESS TEMPERATURE COMBINATIONS

The microwave radiometers measure naturally occurring microwave emission from the Earth's surface and its overlaying atmosphere. Both oceanic and atmospheric physical parameters contribute to the total apparent brightness temperatures measured over the top of the atmosphere by a microwave radiometer. For higher microwave frequencies, the dominant brightness temperature signal contribution comes from the atmosphere. For lower microwave frequencies (36 GHz and lower) the surface signal becomes strong enough to provide for wind speed retrievals using the V or H polarization microwave observation; however, the wind direction signal is very weak. The knowledge of the atmospheric variables is critical if the single polarization is to be used for full wind vector retrieval. Furthermore a small error in the atmospheric corrections will lead to a significant error in the wind direction retrievals.

However with the certain linear combination between the V and H brightness temperatures, the atmospheric correction may not be required. This linear combination was previously found to be mostly independent of the atmospheric parameters and is predominantly a function of the surface wind speed, wind direction and sea surface temperature (SST) (Wentz, 1992; Meissner and Wentz, 2002). The linear brightness temperature combination is expressed as $A T_{BV}$-T_{BH} or simply *A*V-H, where *A* is a constant dependent on microwave frequency used (Jelanak, 2005), and will be discussed below.

From the radiative transfer theory, the total apparent brightness temperature collected at the radiometer antenna may be expressed as (Meissner and Wentz, 2002)

$$T_B = T_{BU} + \tau E T_s + \tau R(1+\Omega)(T_{BD} + \tau T_c) \qquad (1)$$

The T_{BU} and T_{BD} are upwelling and downwelling atmospheric brightness temperature respectively and are given by Meissner and Wentz (2002) in (2)

$$T_{BU} = \int_0^\infty \alpha(z) T(z) \tau(z,S) dz$$
$$T_{BD} = \int_0^\infty \alpha(z) T(z) \tau(0,z) dz \qquad (2)$$

The $\alpha(z)$ and $T(z)$ are the atmospheric absorption and physical temperature profile at altitude z respectively. The atmospheric transmittance between two points in the atmosphere are defined in term of $\alpha(z)$ as

$$\tau(z_1, z_2) = \exp\left(-\int_{z_1}^{z_2} \alpha(z) dz \right) \qquad (3)$$

The τ, defined as $\tau(0,S)$ from (3), in (1) is the total atmospheric transmittance between the sea level and the top of the atmosphere *S*. The emissivity *E* and the reflectivity *R* in related by Kirchhoff's Law as *R=1-E*. The Ω is the relative surface scattering reflection factor due to wind roughen surface. The T_c is the cosmic brightness temperature equals to 2.7 K and T_s is the SST in degree Kelvin.

If the atmosphere is assumed to be homogeneous, that is if the atmospheric absorption is considered constant, and the atmospheric temperature profile $T(z)$ and the sea surface temperature T_s are approximately

equal, an effective system temperature is define as (Meissner and Wentz, 2002)

$$T_{eff} \equiv T(z) \approx T_s \tag{4}$$

By substitute (4) into (2), the (2) reduce to (Meissner and Wentz, 2002)

$$T_{BU} = T_{BD} = (1-\tau)T_{eff} \tag{5}$$

and by substitute (5) into (1), the (1) becomes (Meissner and Wentz, 2002)

$$T_B \approx T_{eff} - R\tau^2 T_{eff} + R\tau(1-\tau)\Omega T_{eff} + (1+\Omega)R\tau^2 T_c \tag{6}$$

The last two terms in (6) are small and negligible and the total apparent brightness temperature simplify to (Meissner and Wentz, 2002)

$$T_B \approx (1-R\tau^2)T_{eff} \tag{7}$$

From (7) the total brightness temperature are a function of surface reflectivity, the atmospheric transmittance and the effective temperature. Let *A* define as the ratio between the V and H surface reflectivity

$$A \equiv \frac{R_H}{R_V} \tag{8}$$

The brightness temperature from (7) can be rewritten in term of R_V as

$$\begin{aligned} T_{BV} &\approx (1-R_V\tau^2)T_{eff} \\ T_{BH} &\approx (1-AR_V\tau^2)T_{eff} \end{aligned} \tag{9}$$

By taking a partial derivative of (9) with respect to τ, (9) becomes

$$\partial T_{BV} \approx -2R_V \tau T_{eff} \partial\tau \tag{10a}$$

$$\partial T_{BH} \approx -A2R_V \tau T_{eff} \partial\tau \tag{10b}$$

Multiply (10a) with *A* and subtract it from (10b), yields, after some rearranging of the terms

$$\frac{\partial(AT_{BV} - T_{BH})}{\partial\tau} \approx 0 \tag{11}$$

This means that the brightness temperature combination AT_{BV}-T_{BH} is invarient with the atmospheric water vapor in low cloud condition.

From (8) the *A* depends on the surface reflectivity at the time of the observation. Since the surface reflectivity is not available, it is not possible to calculate the *A* directly. However, when the brightness temperature combination *A*V-H is substituted with (7), this becomes

$$AT_{BV} - T_{BH} \approx (A-1)T_{eff} - (AR_V - R_H)\tau^2 T_{eff} \tag{12}$$

The second term in (12) is canceled using the relationship from (8); and with some algebra, the *A* is derived as

$$A \approx \frac{T_{BH} - T_{eff}}{T_{BV} - T_{eff}} \tag{13}$$

Here, the T_{eff} is approximated to the sea surface temperature (SST) in degree Kelvin.

For the specular reflection, the reflectivity is a function of frequency, polarization, incidence angle, and the dielectric constant of the seawater, when there is no wind and the sea surface is smooth. However, as the sea surface roughens by the increasing wind speed, the reflectivity gets altered. Since the *A* is defined as the ratio of the reflectivity in (8), the *A* becomes a function of wind speed. In addition, since the dielectric constant of the seawater is a function of the water temperature, foam, white caps as well as salinity, the *A* should also be a function of these parameters; however, only the sea surface temperature was taken into account here.

Given the brightness temperature combination of *A*V-H is independent of the atmospheric transmissivity in (11) and the *A* parameter can be calculated from (13), the *A*V-H relationship is a function of surface parameters: wind speed, wind direction and SST. Therefore an empirical model function can be derived for WindSat's measurements. The model function derivation procedure is describe in detail in the next section.

4. MODEL FUNCTION

In this section, the procedure used to obtain the model function coefficients is described. The model function was found by using a proper mathematical equation to regress the average of *A*V-H measurements in a particular surface parameter bin. This way *A*V-H was defined as a function of appropriate parameter. Here we model the *A*V-H as a function of wind speed, relative wind direction and SST in the following form

$$\begin{aligned} AT_{BV} - T_{BH} = \underbrace{F(SST) + C_0(WSPD)}_{dc} \\ + C_1(WSPD)\cdot COS(\chi) + C_2(WSPD)\cdot COS(2\chi) \end{aligned} \tag{14}$$

The left hand side of (14) is obtained from the measurement. The average values of *A*V-H were found as a function of wind speed and SST from the binned dataset. The average of the last two terms in (14) over all wind direction is zero thus the mean *A*V-H is a function of wind speed and SST.

When a specular reflection is assumed; the surface is smooth and the wind speed is assumed to be zero, the brightness temperature in (14) would be a function of only SST. The initial SST dependence may be found by extrapolating the mean *A*V-H to wind speed equal to zero. The initial SST dependence found was in the mean values for a given SST bin thus a mathematical form that was best decribe the SST dependence in the mean was found. The SST dependent function *F(SST)* was found for the two different data versions (GDAS's SST and WindSat's SST)

The initial *F(SST),* found above, was subtracted from the measured *A*V-H in (14), yeilds

$$\begin{aligned} (AT_{BV} - T_{BH}) - F(SST) = F(WDIR) = C_0(WSPD) \\ + C_1(WSPD)\cdot COS(\chi) + C_2(WSPD)\cdot COS(2\chi) \end{aligned} \tag{15}$$

The average of the remaining of *A*V-H was then

calculated. The mean values were regressed using the two haromic cosine functional form as in (15). The coefficient C_0, C_1 and C_2 were then obtained for each wind speed bin. The *C*'s cofficients are essentially the mean values for given wind speed, and to model them a proper mathematical from was found to fit the mean values. Note that the coefficient C_0 can be thought as wind speed dependent term only. The *C*'s coefficients found here again were derived for the two different versions of the SST bin dataset as described above.

Now an iterative process has been established. The second iteration was started by using the *F(WDIR)* found previously and subtracted it from measured *A*V-H for each version of SST bins and the new *F(SST)* was derived. From the new *F(SST)* found, the new *C*'s coefficient was found using the same procedure found above. The iteration process was repeated until convergence for all coefficients was reached.

The final wind direction variations for different version of SST bins used are shown for selected wind speed in Fig. 1. The *dc* wind speed dependent term was removed from the plots in Fig 1 and is shown separatedly in Fig. 2. Finally the *dc* SST term is shown in Fig. 3. When all terms are added together, an empirical model for *A*V-H brightness temperature is established.

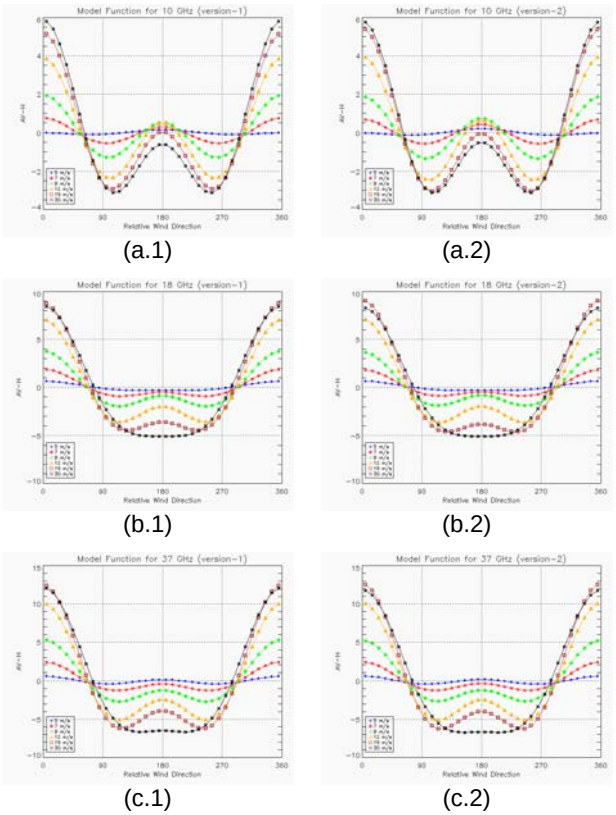

(a.1) (a.2)

(b.1) (b.2)

(c.1) (c.2)

Figure 1: The wind vector model function is shown for three frequency channel: 10, 18 and 37 GHz. The first column is the model derived from version 1 dataset (GDAS'SST) and the second column was derived from version 2 dataset (WindSat's SST)

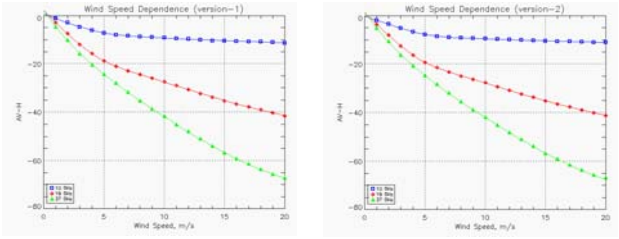

(b)

Figure 2: The *dc* wind speed dependence terms after several iterations. (a).Wind speed dependent for version 1 (b) Wind speed dependent for version 2

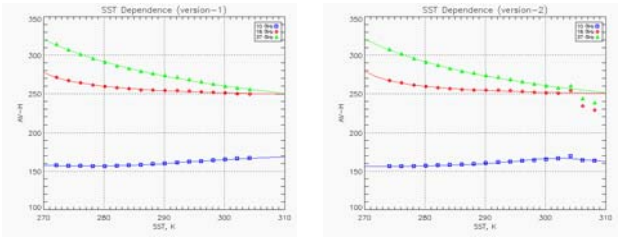

(a) (b)

Figure 3: The *dc* SST dependence terms after several iterations for (a).using GDAS's SST (b) using WindSat's SST

5. CONCLUSION

The wind vector model function has been developed for WindSat radiometer solely from vertical and horizontal polarization brightness temperature measurement. The brightness temperature combination in the form of *A*V-H has proven to be independent of the atmospheric variables and was modeled as a function of surface wind vector and sea surface temperature (SST).

In order to assess usability of WindSat retrieved SST, the model development was based on both WindSat retrieved and GADS SST. The models developed from two different data sets were very similar. This was important conclusion since it will be more desirable to use WindSat retrievals than an external data set in subsequent wind vector retrieval applications of this model.

Eventhough this newly develop wind vector model has relatively stronger wind directional signal than individual polarizations itself, for low to moderate wind speeds, the signal lies within the measurement noise, and thus it would be difficult to derive wind vector solely using this brightness temperature combination. However, in combination with third and fourth Stokes measurements from WindSat, additional directional information will add to the overall wind vector retrieval accuracy.

REFERENCES

Connor L. N. P. S. Chang, Z. Jelenak, N.-Y. Wang and T. P. Mavor (2004): WindSat validation datasets: An overview, *Proc. IGARSS*, 386-389.

Freilich, M. H. And R. S. Dunbar (1993): A preliminary C-band model function for the ERS-1 AMI instrument, *Proc. First ERS-1 Symposium,* **ESA SP-359**, 79-84

Gaiser P. and M. Bettenhausen (2005): The WindSat polarimetric radiometer and ocean wind measurements, *MTS/IEEE Oceans*.

Jelenak, Z., T. Mavor, L. Connor and P. S. Chang (2005): Ocean wind vector retrievals from WindSat polarimetric measurements in extreme events 2004 hurricane season, presented at *Ocean Vector Wind Science Team Meeting.*

Jelenak, Z., T. Mavor, L. Connor, N.-Y. Wang, P. S. Chang, and P. Gaiser (2004): Validation of ocean wind vector retrievals from WindSat polarimetric measurements, presented at *The 4th Int. Asian-Pacific Environmental Remote Sensing Conf.*

Meissner T. and F. Wentz (2002): An updated analysis of the ocean surface wind direction signal in passive microwave brightness temperature, *IEEE Trans. Geosci. Remote Sensing,* **6**

Moore R. K. and W. L. Jones (2004): Satellite scatterometer wind vector measurment — the legacy of the Seasat satellite scatterometer, *IEEE Geosci. Remote Sensing Newsletter,* **132**, 18-32.

Schroeder L. C. et al (1985): Removal of ambiguous wind directions for a Ku-band wind scatterometer using three different azimuth angles, *IEEE Trans. Geosci. Remote Sensing,* **GE-23**, 91-100.

Shaffer S. J., R. S. Dunbar, S. V. Hsiao, and D. G. Long (1991): A median-filter-based ambiguity removal algorithm for NSCAT, *IEEE Trans. Geosci. Remote Sensing,* **29**, 167-174

Wentz F. (1992): Measurement of oceanic wind vector using satellite microwave radiometer, *IEEE Trans. GeoSci. Remote Sensing,* **30**, 5.